



## Short Review

## Melting points of ionic liquids: Review and evaluation

Zhengxing Dai<sup>1,2</sup>, Lei Wang<sup>1</sup>, Xiaohua Lu<sup>1,\*</sup>, Xiaoyan Ji<sup>2,\*</sup><sup>1</sup> State Key Laboratory of Material-Oriented Chemical Engineering, Nanjing Tech University, Nanjing, China<sup>2</sup> Energy Engineering, Division of Energy Science, Luleå University of Technology, Luleå, Sweden

Received 9 November 2023; revised 11 January 2024; accepted 31 January 2024

Available online ■ ■ ■

## Abstract

The melting points of ionic liquids (ILs) reported since 2020 were surveyed, collected, and reviewed, which were further combined with the previous data to provide a database with 3129 ILs ranging from 177.15 to 645.9 K in melting points. In addition, the factors that affect the melting point of ILs from macro, micro, and thermodynamic perspectives were summarized and analyzed. Then the development of the quantitative structure-property relationship (QSPR), group contribution method (GCM), and conductor-like screening model for realistic solvents (COSMO-RS) for predicting the melting points of ILs were reviewed and further analyzed. Combined with the evaluation together with the preliminary study conducted in this work, it shows that COSMO-RS is more promising and possible to further improve its performance, and a framework was thus proposed.

© 2024 Institute of Process Engineering, Chinese Academy of Sciences. Publishing services by Elsevier B.V. on behalf of KeAi Communications Co., Ltd. This is an open access article under the CC BY-NC-ND license (<http://creativecommons.org/licenses/by-nc-nd/4.0/>).

**Keywords:** Ionic liquids; Melting point; COSMO-RS; QSPR; GCM

## 1. Introduction

Ionic liquids (ILs) are solvents with salt structures containing cations and anions [1-2]. ILs have received much attention from industry and academia because of their advantages, such as desirable electrical conductivity, non-volatility, high thermal stability, and so on [3-4]. They have been developed for applications in different areas like energy storage, separation, electrochemistry, and catalysis [5-6]. In different applications, the operational conditions, i.e., pressure and temperature, are quite different, which would affect the state of ILs. The melting point can be used to judge the fluid state, and its value is important information when using and developing ILs for a specific application [7].

Usually, the melting points can be measured experimentally [8-10]. For ILs, as one of the important properties, their

melting points have been determined extensively, and reviewing them to establish a database is important to select suitable ILs for different applications. To the best of our knowledge, the melting points of ILs were collected but for the purpose of model development, and no work has been conducted to summarize the available melting points of ILs specifically. Also, the number of ILs has rapidly increased recently, calling for reviewing the melting points of ILs and updating the available database.

The melting point can also be obtained theoretically, which is particularly desirable for ILs. The designable nature of ILs indicates that more and more ILs will be created in the future. On the one hand, measuring the melting points of new ILs one by one is time-consuming. On the other hand, as the number of ILs that can be potentially synthesized can be up to  $10^{18}$ , experimental determination is impractical. Thus, developing a model, especially a predictive one is essential. Models, such as the quantitative structure-property relationship (QSPR), the group contribution method (GCM), and the conductor-like screening model for realistic solvents (COSMO-RS) have been

\* Corresponding authors.

E-mail addresses: [xhlu@njtech.edu.cn](mailto:xhlu@njtech.edu.cn) (X. Lu), [Xiaoyan.ji@ltu.se](mailto:Xiaoyan.ji@ltu.se) (X. Ji).

developed to predict the melting points of ILs [11-13]. However, which model is better, and how to further improve and develop models are still unclear, calling for reviewing, understanding, and analyzing the available work.

This work was to review the melting point of ILs via an intensive literature survey, both on the melting points of ILs determined experimentally and on the models in describing or predicting them. More specifically, in this work, according to the literature survey, the newly determined melting points of ILs published since 2020 were collected and summarized, and the collected data together with the available data collected in other research articles were further analyzed to investigate how different factors, including the microstructures of ILs, affect their melting points. In parallel, the models were reviewed, assessed, and analyzed, and the framework for further developing predictive models was provided.

## 2. Data review, collection, and analysis

A literature survey was conducted extensively to collect the melting points of ILs. It shows that the melting points of ILs published before 2020 have been collected and used as the database in the work by Mital et al. [14] and Venkatraman et al. [15]. Therefore, the data in the open publications since 2020 was further collected, covering 584 ILs. The newly collected experimental results are summarized in Table S1, together with the full names of ILs.

The newly collected data and those collected in the published articles were further analyzed and compared. In Table 1, the summary of collected data in this work and those in the work by Mital et al. [14], and Venkatraman et al. [15] is provided. It shows that the data with a wide range of melting points collected by Venkatraman et al. covers 2212 ILs; the data collected by Mital et al. includes 1260 ILs, and compared with the former, 333 new ILs are newly added; the data collected in this work contains 610 ILs, among them, 584 ILs are new. According to Table 1, the melting points of 3129 ILs have been reported, the lowest and largest melting points among 4507 data points are 177.15 K and 645.9 K, respectively, which can be found in the work of Gupta et al. and González-Izquierdo et al. [16-17].

Actually, an IL has only one melting point. However, the number of data point is larger than that of ILs, as listed in Table 1. This is because that the melting points of the same ILs in different literatures were collected. The experimental deviation of some ILs is high when comparing the melting points of an IL from different references. For example, the melting points of 1-Butyl-3-methylimidazolium bis ((trifluoromethyl)

sulfonyl)imide measured by Agafonov et al. (275.15 K) and Wang et al. (219.15 K) are quite different, and their deviation is 25.55% [18-19]. As we know, the model development and verification are all based on the experimental data, and the used experimental data will affect the result. Therefore, a comprehensive collection and evaluation of melting points of ILs is important.

During the determination of melting points, the properties of ILs, such as density, viscosity, and conductivity, were reported, and the effect of different impactors, especially the microstructure of ILs, on the melting points was also investigated. This is essential considering the huge number of ILs, and such an investigation will also provide valuable information for developing models.

ILs consist of cations and anions (i.e., IL-ions), and their properties strongly depend on them. The effect of IL-ions on the melting points has been intensively studied. From the aspect of the effect of IL-cations, Liu et al. found that the melting points of 1-methyl-3-ethylacetate-1,2,4-triazolium-based ILs change in the order of  $[NTf_2]^+ < [NO_3]^+ < [Cl]^+$  [20]. The melting points of ILs increasing with the order of  $[BF_4]^- < [PF_6]^- < [ClSal]^-$  has been found by Diabate et al. [21]. Langtry et al. pointed out that the ILs containing the  $[NTf_2]^+$  anion have lower melting points compared to their  $Br^-$ ,  $[PF_6]^-$ , and  $[BF_4]^-$  counterparts [22]. Also, the effect of the substituent groups in IL-anion has been discussed. Myrdek et al. evidenced that the propoxyethylene groups present in the anions can lower the melting point, which is in line with the published "Concept of Melting Point Lowering due to Ethoxylation" [23].

Similarly, the effect of IL-cations has been discussed, including the substituent groups in IL-cation and the alkyl chain length of IL-cation. For the substituent groups in IL-cation, O'Brien et al. revealed that cyclopropane as an unsaturation "effect isostere" can lower the melting points in the lipid-like ILs [24]. Warrington et al. mentioned that the inclusion of an alkoxy group typically lowers the melting point [25]. Lerch and Strassner found that the ILs with fluorinated moieties in para-position have higher melting points than their non-fluorinated homologs, and this trend is reversed for the ILs with ortho-substituted methoxy groups [26]. The research of Río et al. shows that ILs featuring unsaturated alkyl tails exhibit a low melting point [27]. For the alkyl chain length of IL-cation, two organic cations  $[Bu_3NC_2NHC_n]^+$ -based ILs ( $n=4$  or  $8$ ) were researched by Diabate et al., and they found that the melting point increases with increasing the alkyl chain length [21]. However, Peppel and Kockerling obtained that the melting points of the hexaisothiocyanato complexes can be

Table 1  
The summary of the collected melting points of ILs.

No.	Melting points (K)	Number of data points	Number of ILs	Number of additional ILs	Ref. & published year
1	188.15-645.9	621	610	584	This work
2	201.15-581.6	1674	1260	333	[14] & 2021
3	177.15-632.15	2212	2212	0 (Base)	[15] & 2018

lowered by extending the length of the alkyl chain in the imidazolium-based cation [28]. Interestingly, Kawai et al. uncovered that the melting point of  $[2C_n(2-O-2)][NTf_2]$  decreased as the alkyl chain length increases from  $C_{10}$  to  $C_{12}$ , whereas an increase in the alkyl chain length from  $C_{12}$  to  $C_{14}$  significantly increases the melting point [29]. Darabi and Zare found that the melting point of  $[C_nmim]I$  decreases from  $n=2$  to  $n=4$  and increases from  $n=4$  to  $n=8$  [30]. Moreover, Lerch and Strassner pointed out that there are no general trends of melting point versus the alkyl chain lengths [26]. Based on the microstructure of ILs, the effect of alkyl chain lengths was clarified. Turner et al. found the balance between the coulombic and the van der Waals interactions controlling the melting point of the ILs with different alkyl chain lengths [31]. Darabi and Zare found that the coulomb force dominates when the alkyl chain of ILs is short; with increasing alkyl chain length, the competition between the coulomb force and dispersion interaction emerges [30].

Indeed, different anions and cations bring complex microstructures of ILs. Therefore, many researchers have analyzed the melting points from the microstructure of ILs. Cassity et al. found that increasing the dipole moment of the IL-cation lowers the melting point of ILs [32]. Rabideau et al. tuned the melting point of ILs by adjusting the dipole moment of IL-cations but drew an opposite conclusion, i.e., the cations with higher dipole moments generally have lower melting points [33]. Zakharov et al. mentioned that the melting point depends on the number of hydrogen bonds [10]. Khalili et al. thought that the hydrogen bond can act as a defect in the coulomb networks of ILs to decrease the melting point of ILs [34]. However, Mydrek et al. proposed that the presence of hydrogen bonds in ILs will increase the melting point [23]. The effects of other interactions in ILs have also been discussed. Chen et al. thought that the low melting points could be attributed to a weak coulomb force, and dihydrogen bonding can enhance the attraction between cations and anions to increase the melting points [35]. Clarke et al. mentioned that the prevented  $\pi-\pi$  stacking can decrease the melting points of the  $[NTf_2]^-$  ILs. According to the above discussion, we can summarize that the interaction of ILs will affect their melting points, but the relationship between a particular force/interaction and melting point is controversial, and different interactions jointly affect the melting points. Besides, from a thermodynamic view, the enthalpy is the sum of the internal energy for a system, and Rabideau et al. believed that reducing the liquid enthalpy would lower the melting point of ILs [33].

It is well known that the molecular packing density in the crystal lattice is a major factor affecting the melting point of the compound [36], which has been used to analyze the melting points of ILs. In the work by Warrington et al., it was pointed out that the presence of ether oxygen increases the polarity and flexibility of the cation, causing less efficient packing and lowering the melting point of ILs [25]. The X-ray crystallography of ILs was conducted by Sumitani et al., and it was found that a relatively high melting point of ILs was caused by the dense molecular packing [37]. Niemczak et al.

also mentioned that the polar C–I bond in the investigated ILs creates a molecular dipole, which favors better packing, eventually increasing the melting point [38]. Hence, the dense molecular packing will increase the melting points of ILs.

To lower the melting point of ILs, the molecular packing of ILs needs to be reduced. Thus, the factors affecting the molecular packing of ILs are discussed here. (1) More symmetrical molecules were found to provide denser packing [36, 39], and the ILs with asymmetrical structures always have low melting points [37, 40–45]. (2) The size of IL-ions also affects the molecular packing. Warrington et al. thought smaller cations allow for more efficient packing of the ions so that the lower melting point for the  $[TFSI]^-$  ILs may be due to the larger size of  $[TFSI]^-$  compared to  $[FSI]^-$  [25]. Fabre et al. and Huang et al. also mentioned that the larger the anion size, the lower the melting point [42, 46]. Liu et al. found that a larger volume of IL-anions results in a lower melting point [47]. (3) Conformation affects the packing of ILs as well. Zafar et al. found that adding conformation degrees of freedom decreases the molecular packing and melting point [45]. In the work by Yoon et al.,  $[N_{111}(1O2)][FSI]$  was found to have a lower melting point than  $[N_{111}(2O1)][FSI]$  because of its high conformational flexibility [39]. In summary, the packing density of ILs plays an important role in affecting the melting point of ILs. The symmetry, size, and conformational degree of freedom affect the packing density. In the statistical mechanics, entropy is a measure of "disorder" in a system (the higher the entropy, the higher the disorder) [48], and Endo et al. reported that entropy plays a deterministic role in lowering the melting point of ILs [49].

According to the literature survey, many factors affect the melting points, which was further summarized as illustrated in Fig. 1. Obviously, it is insufficient to analyze the melting point with IL-cations and IL-anions from a macro perspective, calling for a complicated analysis with different energies and structures from a micro perspective, while from a thermodynamic perspective, the melting points can be easily analyzed by entropy and enthalpy.

### 3. Modelling: summary and analysis

In contrast to the model developed for describing the properties of ILs, only a very limited number of models have been developed to describe the melting points of ILs, and they are QSPR, GCM, and COSMO-RS [50–53].

#### 3.1. QSPR

The QSPR method is based on the idea that all physical properties of a compound are directly related to its chemical structure [54]. Katritzky et al. extended the QSPR model from organic compounds to the pyridinium bromide ILs using six descriptors generated by the CODESSA program [55]. Then the QSPR models for the ILs with different series of nitrogen-containing organic cations, such as imidazolium bromides [56], chlorides [57], tetrafluoroborates and hexafluorophosphates [58],

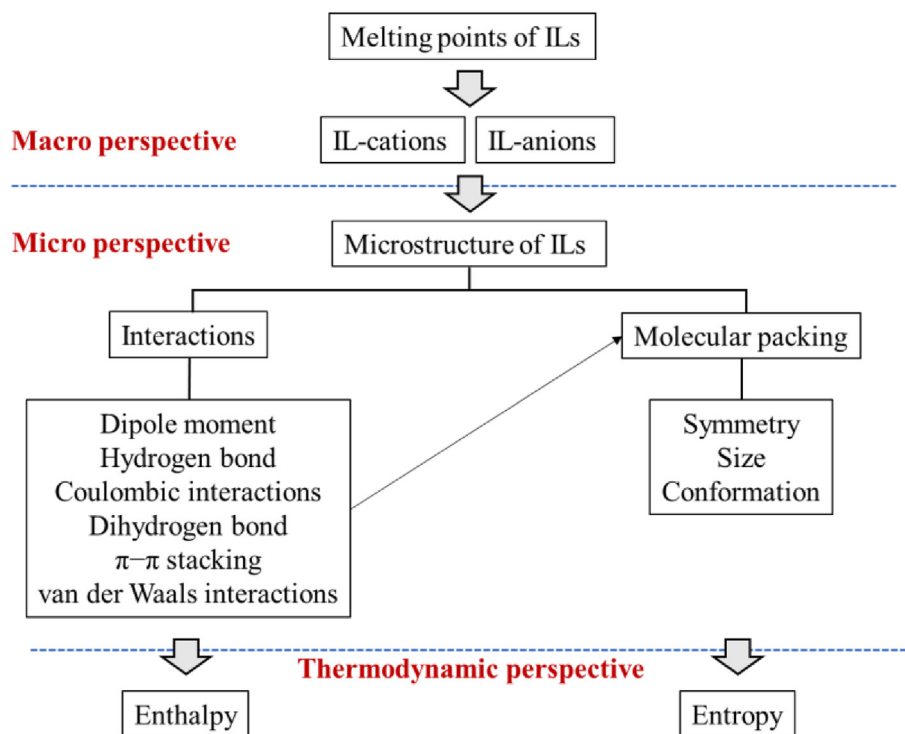


Fig. 1. The factors influencing the ILs melting points.

benzimidazolium bromides [59], and quaternary ammonium [54], were developed. However, all these QSPR models account for the effect of cation only. Later, the QSPR model was further developed to consider the anion and cation effects in describing imidazolium ILs [60–61] and other diverse classes of ILs [62]. After that, the interaction of anions and cations was also considered as descriptors to predict the melting points of 394 ILs [50, 63]. It can be easily found that the types of descriptors in the QSPR model are more and more, which are similar to factors summarized in Fig. 1, with the development of QSPR.

The QSPR models proposed are listed in Table 2. It can be noticed that the development of the QSPR models is quite independent, i.e., each QSPR model is almost new, and no one is based on the previous ones; the early developed QSPR model used fewer descriptors to model some specific ILs, i.e., different QSPR models were developed for different series of ILs. For example, the QSPR models for N-pyridinium bromide ILs and tetraalkyl-ammonium bromide ILs are different, and more importantly, the descriptors are also different [54]. Introducing more descriptors obtained from more kinds of software and more advanced regression techniques combined with machine learning, a universal QSPR model can be proposed to describe the melting points of ILs. However, when using different databases, different descriptors, and/or different regression techniques, the “universal” QSPR models are indeed different, not universal anymore. Besides, it is difficult to give explicit expressions for any QSPR models [15, 50], challenging to reproduce and evaluate which QSPR model is better.

Recently, a new QSPR model was proposed by Padaszynski et al. [50], where 45 types of molecular descriptors were used and the melting points of 953 ILs were studied. In this work,

the average absolute relative deviation (AARD) of each family of cations and anions ranges from 2.6 to 13.3 %, and it was stated that 80 % accuracy originates from the upper limit of modern machine learning approaches. The large database and advanced regression techniques improve the performance of the QSPR model, while it will become more complex as more descriptors are used. Although the QSPR model has shortcomings as a typical data-driven machine learning model, it should be pointed out that it can be used to find out the important factors that affect the melting points. For example, despite the QSPR model limitations, Lopez-Martin et al. found the most important impactors are size, symmetry, and charge distribution in either the cation or the anion when modeling the melting points of ILs [60].

### 3.2. GCM

GCM is another model to describe the melting points of ILs. In this model, the structural-functional groups of a compound define the contributions toward the overall melting point, and it was considered as a special case of a QSPR model because the functional groups in GCM can be used as descriptors in a QSPR model [64]. The development of GCMs for ILs is similar to the QSPR models. The first GCM for predicting the melting points of ILs was an extension of GCM from organic compounds, where only imidazolium- and benzimidazolium-based ILs were studied [65]. Later, this model was extended to a diverse series of ILs [7, 66–68]. The used equations on GCM are almost the same, indicating that the research on GCM is continuous, which is different from the QSPR model.

Table 2  
Summary of the QSPR models for the IL melting points.

ILs databases, descriptors, and models	Software to generate descriptors	Regression techniques	Ref
Set A - 57 imidazolium ILs: $T_m = - (62.02 \pm 6.16)E_{HOMO-LUMO} + (96.58 \pm 14.68)J + (1482.1 \pm 232.1)P_\mu + (667.4 \pm 141.7)Q_{max,N} - (8.17 \pm 1.89)E_{max,e-n,C-N} + (9.45 \pm 3.56)$ Set B - 29 imidazolium ILs: $T_m = - (14.04 \pm 2.07)E_{max,e-n,C-N} + (0.905 \pm 0.138)HDSA1_{HA} + (3.69 \pm 0.71)N_H + (51.16 \pm 15.02)S - (341.5 \pm 122.2)Q_{max,O} + (4513 \pm 655)$ Set C - 18 imidazolium ILs: $T_m = - (25.78 \pm 1.82)RNCS + (4.52 \pm 0.36)HDSA1_{HA} - (10.3 \pm 1.40)E_{min,C-N} + (3027 \pm 426)$ Set D - 45 benzimidazolium ILs: $T_m = - (224.4 \pm 34.3)E_{c(C-H)} + (0.74 \pm 0.15)HDSA + (45.3 \pm 9.6)E_{min,ex(C-C)} - (12.04 \pm 2.95)RPCS - (1752 \pm 607)R_{Emax,C} + (1015 \pm 142)$	CODESSA	Heuristic or the best multilinear regression method	[56]
Set A - 126 N-pyridinium bromides ILs: $T_m = 125.846 + 0.5773446[PNSA_2] - 2273.22[FNSA_3] - 104.034[BIC] + 254.703[RNCG] - 74.3734[RPCS]$ Set B - 75 Tetraalkyl-ammonium bromides ILs: $T_m = 119.32 + 1841.668[\chi_c - \chi_c^V] + 6.598[I_{adj}^M] + 120.51[CIC] - 124.9688[\chi^V] - 65.08[\Phi]$ Set C - 34 (n-Hydroxyalkyl)-trialkyl-ammonium bromides ILs: $T_m = 5072.73 + 1239.11[\chi_c^V] - 240.719[IC] + 10457.4[\chi^V] + 3499.28[\chi^V] - 6783.74[SC_1]$	CODESSA	genetic function approximation	[54]
A diverse set of 288 ILs including pyridinium bromides, imidazolium bromides, benzimidazolium bromides, and 1-substituted 4-amino-1,2,4-triazolium bromides: By Heuristic method (linear model): $T_m = (99.59 \pm 7.52)[N_{BR}] + (19.77 \pm 1.92)[N_{AB}] - (458.92 \pm 59.38)[RN_{SB}] + (16.41 \pm 4.36)[\chi^V] + (69.46 \pm 9.86)[J] - (10.62 \pm 1.51)[\#H_f] - (1218.20 \pm 207.74)[N_{Avg}(N)] - (15.69 \pm 3.37)[E_{en}(C-H)] - (624.78 \pm 210.54)$ By Pursuit regression (nonlinear model): The expression of equation wasn't given	CODESSA	Heuristic Method and Projection Pursuit Regression	[59]
808 diverse ILs belongs to Sulfonium, Ammonium, Pyridinium, 1,3-Dialkyl imidazolium, Tri-alkyl imidazolium, Phosphonium, Pyrrolidinium, Double imidazolium, 1-Alkyl imidazolium, Piperidinium, Pyrroline, Oxazolidinium, Amino acids, Guanidinium, Morpholinium, Isoquinolinium and Tetra-alkyl imidazolium: $T_m = (959.6153 \pm 45.8285) + (24.6002 \pm 4.8970)[Mor08p]^{Cation} - (48.6747 \pm 8.8114)[MATS4v^{Cation}] - (244.665 \pm 24.8857)[MATS1m^{Cation}] - (64.139 \pm 11.4208)[Mor29u^{Cation}] - (656.913 \pm 62.5673)[X1A^{Cation}] - (33.6686 \pm 4.3378)[IC2^{Cation}] + (0.1780 \pm 0.0146)[t - veVSA^{Cation}] - (21.2957 \pm 5.2520)ATS7e^{Cation} - (468.943 \pm 54.5890)[X0Av^{Anion}] - (2.4326 \pm 0.4928)[nX^{Anion}] + (0.2066 \pm 0.0866)[AMW^{Anion}] + (0.0225 \pm 0.0028)[tNPSA^{Anion}]$	Sarchitect	Genetic Function Approximation	[62]
394 ILs (120 imidazolium, 43 benzimidazolium, 109 pyridinium, 19 pyrrolidinium, 65 ammonium, 7 sulfonium, 20 triazolium and 11 guanidinium 36, 36, and 9 descriptors used for cations, anions and their interaction respectively The expression of equation wasn't given	General topological index	Multiple linear regression	[63]
2212 ILs (1369 cations and 141 anions) For different regression the number of descriptors(parameters) ranges from 19-104 The expression of equation wasn't given	PM6, MarvinSketch, OpenBabel, KRAKENX	Partial Least Squares Regression, Support Vector Regression, Random Forests Regression etc.	[15]
953 ILs (22 and 14 chemical families of cations and anions) 45 types of molecular descriptors The expression of equation wasn't given	CODESSA, DRAGON	multiple linear regression, partial least squares regression	[50]

GCM can be divided into two categories. One is expressed as eq. (1), where  $N_{ai}$ ,  $N_{ci}$ ,  $T_{mai}$ ,  $T_{mci}$ ,  $N_a$ , and  $N_c$  represent the number of occurrences of the  $i$ th functional group, the contribution of the  $i$ th sub-structure, and the number of total sub-structure of anions and cations, respectively.  $T_{m0}$  is the intercept.

$$T_m = \sum_{i=1}^{N_a} N_{ai} T_{mai} + \sum_{i=1}^{N_c} N_{ci} T_{mci} + T_{m0} \quad (1)$$

This category is the simplest GCM [69], where only cations and anions are considered in the modelling. Recently, Mital et al. critically evaluated and refined the existing GCMs in

predicting the melting points of ILs, and they pointed out that the early-developed GCM models are insufficient in predicting the melting point of new ILs with the original functional group parameters [14]. After re-parametrizing based on the new database with 933 ILs, the AARD of GCM decreased from 13.98 to 9.66 %. This implies that the performance of GCM depends on the experimental database used in parameterizing, i.e., the prediction capability of GCM is insufficient. Compared with QSPR, this type of GCM provides simple and explicit expressions, and the descriptors are only cations and anions. However, in this category of GCM, other impactors, such as the different interactions between each functional group, has not been considered, which might be the reason for a relatively high deviation in predicting the melting points of some ILs.

The other GCM is expressed as eq. (2) [70], where  $n_i$  is the number of the group  $i$  in the molecule,  $T_{m,i}$  is the contribution of group  $i$  to the melting points,  $\sigma$  is a symmetric number determined by the structure of the molecule, and  $\tau$  is the torsional degree of freedom determined by eq. (3).

$$T_m = \frac{\sum n_i T_{m,i}}{A + B\sigma + C\tau} \quad (2)$$

$$\tau = SP3 + 0.5(SP2) + 0.5(RING) - 1 \quad (3)$$

In eq. (3)  $SP3$  and  $SP2$  are the numbers of non-ring, non-terminal  $sp^3$  and  $sp^2$  atoms, and  $RING$  is the number of single rings connected to the system in the molecule. The detail to obtain  $\sigma$  and  $\tau$  can be found in reference [71]. This category of GCM is combined with molecular geometry [70] with a theoretical background of thermodynamics, i.e., the free energy of transition is equal to zero when the phases are in equilibrium, as shown in eq. (4),

$$T_m = \frac{\Delta H_m}{\Delta S_m} \quad (4)$$

where  $\Delta H_m$  and  $\Delta S_m$  are the enthalpy and entropy of transition.

Here, GCM is used to describe the enthalpy of transition in eq. (2), and the entropy of transition is estimated by modifying the Walden's rule [71]. Aguirre et al. used this type of GCM to estimate the melting point of 136 ILs, and the AARD is 7.8% [7]. However, no further work was conducted with a large IL database to verify this method. Based on the analysis of the former type of GCM, we can infer that this method will also be insufficient in predicting the melting point of new ILs, since the enthalpy of transition is derived from GCM instead of dissecting and representing the contribution of the different interactions in enthalpy.

### 3.3. COSMO-RS

The development of COSMO-RS is based on quantum chemistry and statistical thermodynamics. Based on solvation thermodynamics and computational quantum mechanics, COSMO-RS has been widely used to study physicochemical

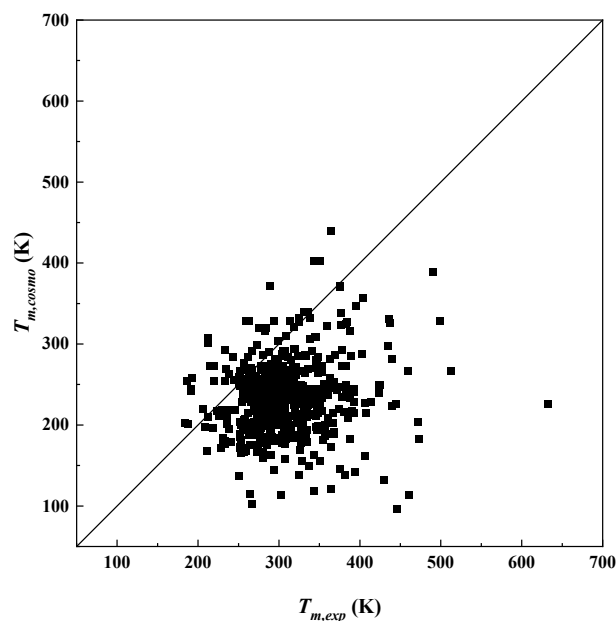


Fig. 2. Comparison between  $T_{m,COSMO}$  and  $T_{m,exp}$ .

properties, for example, volume, area, misfit interaction enthalpy ( $H_{MF}$ ), H-bond interaction enthalpy ( $H_{HB}$ ), and the van der Waals interaction enthalpy ( $H_{vdW}^0$ ), etc. Based on these properties predicted with the first-principle theory in COSMO-RS, the melting points of ILs can be predicted with eq. (5),

$$T_m = \frac{cr_m^3 + dH_{vdW}^0 + eH_{ring}}{aln\sigma + b\tau + 1} \quad (5)$$

where  $H_{ring}$  (the ring interaction enthalpy) and  $H_{vdW}^0$  are calculated with COSMO-RS as the sum of the single-ion enthalpies in a 1:1 mixture of cation and anion at 25°C,  $r_m$  is the mean IL radius, and  $\sigma$  and  $\tau$  are the same as in eq. (2). The detail to obtain  $\sigma$  and  $\tau$  of ILs can be found in reference [72].

The universal constants ( $a$ ,  $b$ ,  $c$ ,  $d$ ,  $e$ ) were obtained from the fitting of the melting points of 67 ILs [72]. All of these have been embedded in the software COSMOtherm. It can be considered as the further development of eq. (2), where the enthalpy of transition is described by  $r_m$ ,  $H_{ring}$  and  $H_{vdW}^0$ . This model can also be seen as a simple QSPR model, where the variable in eq. (5) comes from the computational quantum mechanics, can be used as descriptors.

The performance of COSMO-RS in predicting the properties of ILs, including 39 different cations and 10 different anions, was verified via the comparison of the available experimental data [72], however, no more work has been conducted for other ILs. Therefore, in this part, the performance of COSMO-RS was further evaluated using the software COSMOtherm (version 21.0.1) in the "Ionic Liquids

Table 3  
The refitted coefficients of eq. (5).

a	b	c (nm <sup>-3</sup> )	d (mol·kJ <sup>-1</sup> )	e (mol·kJ <sup>-1</sup> )
-0.1054	0.0769	368.5058	-4.2655	2.7482

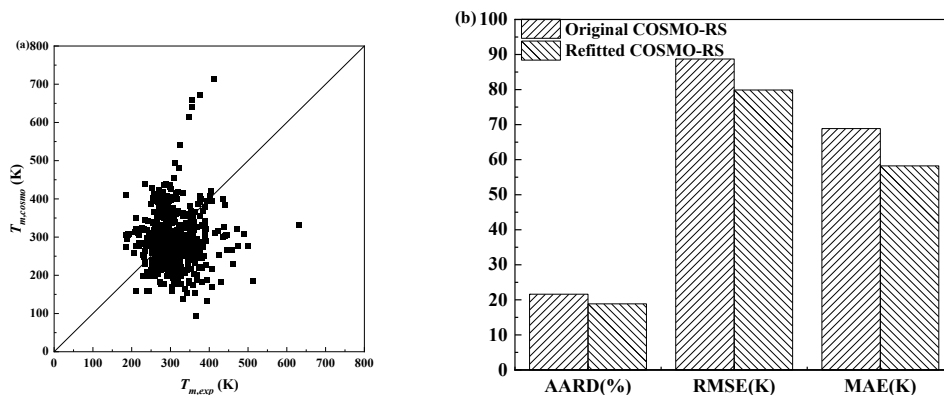


Fig. 3. a) Comparison between the calculation using refitted eq. (5) and the experimental melting points, b) comparisons of AARD, RMSE, and MAE.

Properties” model, where the TZVP level was selected, and the COSMOfiles for all cations and anions of ILs were taken from the COSMOtherm database. Because of the limited number of ILs in the database of COSMOtherm, 529 ILs (including 130 cations and 87 anions) out of 3129 reviewed ILs, were used to verify the performance of COSMO-RS. The predictions ( $T_{m,COSMO}$ ) together with the experimental melting points ( $T_{m,exp}$ ) of 529 ILs are listed in Table S2 and displayed in Fig. 2. The full name and structure of 529 calculated ILs are listed in Table S3 and Table S4. The AARD (21.60%) of CORMO-RS is higher than the original GCM in predicting new ILs (AARD = 13.98 %) (Mital et al., 2021). The higher AARD of CORMO-RS might be caused by the following reasons: 1) the universal constants obtained from 67 ILs in eq. (5) are unsuitable for all ILs; 2) the variables used in eq. (5) to describe the enthalpy of transition is not enough compared with the impactors of melting points summarized in Fig. 1.

In short, the QSPR model proposed by Paduszynski et al. [50] shows that the average absolute relative deviation of each family of cations and anions ranges from 2.6 to 13.3 %. The GCM used by Aguirre et al. represents an average relative deviation of 7.8% [7]. The ARDs of the original and best-modified COSMO-RS in this work are 21.6% and 11.82%. The accuracies of QSPR and GCM are higher than COSMO-RS. However, GCM and COSMO-RS are easier to use and with more theoretical backgrounds than QSPR. Comparing COSMO-RS with GCM, COSMO-RS shows worse predictions than GCM, while different interactions have been used to describe the enthalpy of transition, rather than just attributing it to the contributions of anions and cations.

Table 4  
The modified equations used to improve the performance of the original COSMO-RS.

Additions	Modified equations
$M_w$	$T_{m,COSMO} = \frac{c_r^3 + dH_{vdW}^0 + eH_{ring} + fM_w}{aln\sigma + b\tau + 1}$
$H_{MF}$	$T_{m,COSMO} = \frac{c_r^3 + dH_{vdW}^0 + eH_{ring} + fH_{MF}}{aln\sigma + b\tau + 1}$
$H_{HB}$	$T_{m,COSMO} = \frac{c_r^3 + dH_{vdW}^0 + eH_{ring} + fH_{HB}}{aln\sigma + b\tau + 1}$

Refitting the parameters of eq. (5) to a large IL database can be one strategy to improve the model performance of COSMO-RS. Besides, COSMO-RS can also act as a QSPR model by adding more key descriptors into eq. (5) and using advanced regression techniques with the help of machine learning to further improve.

#### 4. Further discussion and improvement of model prediction

In the former section, the possible reasons for the high deviation of COSMO-RS were mentioned. In this section, two options were selected to improve the performance of COSMO-RS.

Firstly,  $T_{m,exp}$  and  $r_m$ ,  $H_{ring}$ ,  $H_{vdW}^0$ ,  $\sigma$ , and  $\tau$  of 529 ILs obtained from COSMO-RS listed in Table S5 were used to refit the constants in eq. (5). The refitted constants are listed in Table 3, and the AARD of COSMO-RS is reduced to 18.85 % but the largest ARD increased to 120.69 % as shown in Fig. 3 and Table S4. In addition, the root mean square error (RMSE) and the mean absolute error (MAE) of the original COSMO-RS and refitted COSMO-RS were calculated. The RMSE is reduced from 3.26 to 2.94 K and MAE is also reduced from 68.86 to 58.22 K as shown in Fig. 3 and Table S8.

This shows that incorporating more ILs to get more reasonable parameters improved the model performance, while some physical characteristic variables are still missing when describing the enthalpy of transition, causing relatively high deviation for some ILs. Identifying the missing characteristic variables describing the enthalpy of transition is more important for further developing COSMO-RS to predict the melting points of ILs reliably.

To prove this concept, a physical characteristic variable was incorporated into the original COSMO-RS model within 3 modified equations listed in Table 4, in which, the physical characteristic variable is selected based on the factors influencing the ILs melting points summarized in Fig. 1. The modified models were fitted to 529 ILs. Among these three options, adding  $H_{MF}$  is the best, and the AARD, RMSE, and MAE are as low as 11.82%, 1.98 K, and 36.34 K as shown in Fig. 4. The results of the other two are shown in Fig. S1, while

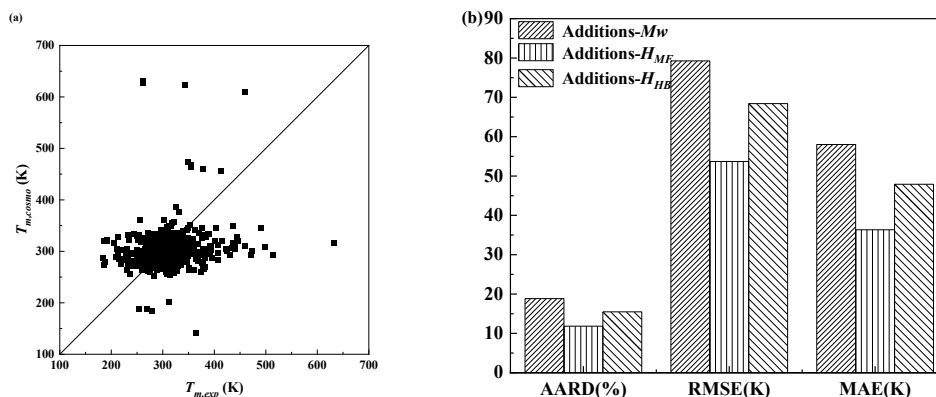


Fig. 4. a) Comparison between the calculation by adding  $H_{MF}$  in eq. (5) and experimental melting points, b) comparisons of AARD, RMSE, and MAE.

$M_w$ ,  $H_{MF}$ , and  $H_{HB}$  of 529 ILs and corresponding parameters and predictions of these 3 corrected equations are summarized in Tables S5–S7. However, still, the largest relative deviation is 141.31%, which is higher than the original COSMO-RS. This means more physical characteristic variables need to be considered to develop COSMO-RS as a quantitative model, and identifying the key physical characteristic variables is the most important issue.

Based on a more preliminary study here, we proposed a framework for the first option (Method 1) as shown in Fig. 5. Here, in Method 1, more physical characteristic variables will be taken from COSMO-RS to further modify the original COSMO-RS and then verify the result with the experimental data. In this work, we only add one physical characteristic, i.e.,  $M_w$ ,  $H_{MF}$  or  $H_{HB}$  into the original COSMO-RS to modify it. Actually, the other physical characteristics provided by COSMO-RS can be added at the same time. For example, we can add  $M_w$  and  $H_{HB}$  into the original COSMO-RS at the same time, not just  $M_w$  or  $H_{HB}$ . Besides the physical characteristic variable mentioned in this work, the dipole moment provided

by COSMO-RS also can be considered according to the impactors of melting points summarized in Fig. 1.

Meanwhile, the above analysis shows that more physical characteristic variables need to be considered, and a lot of physical characteristic variables can be predicted reliably from COSMO-RS. As mentioned above, the COSMO-RS is linked to the QSPR model because the variable in the original COSMO-RS comes from the computational quantum mechanics, and can be used as descriptors. This makes it desirable to develop a hybrid model, i.e., COSMO-RS + machine learning. However, as analyzed before, machine learning will cause the equation complex and even difficult to give explicit expressions. To avoid this, we can use the advantage of machine learning to help us find the ignored key physical characteristic variables and analyze the effect of the current physical characteristics considered in the original COSMO-RS [60]. In addition, using the value deviated from the physical model as the output feature of the machine learning model has been proposed recently [73]. Thus, a framework was also proposed (Method 2). Here we can take the original COSMO-

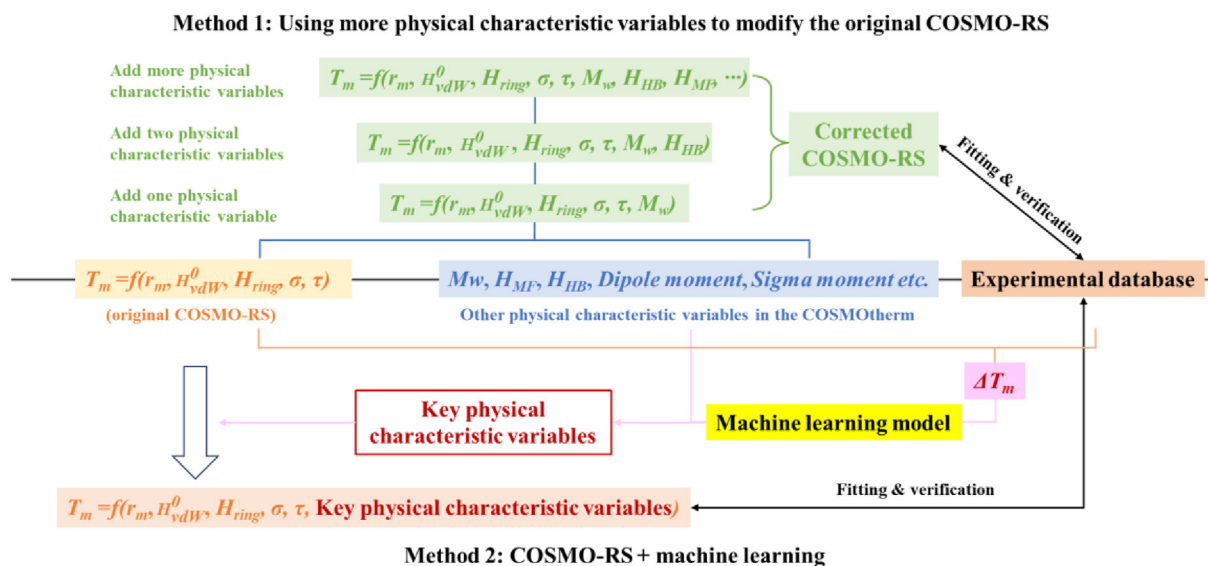


Fig. 5. A framework for improving model performance.



RS model as a physical model and use it to obtain the difference with experiment data. Then we use the machine learning model to help us find the relationship between ignored physical characteristic variables and the differences, helping us to find out the ignored key physical characteristic variables in the original COSMO-RS for further modification of the original COSMO-RS model.

## 5. Conclusions

In this work, the melting points of 3129 ILs were summarized ranging from 177.15 to 645.9 K. In addition, the factors that affect the melting points of ILs were reviewed and analyzed. It is difficult to understand the effect of melting points by cations and anions only from the macro perspective, without considering the interactions between cations and anions from the micro perspective. The interactions of ILs is complex, which cause the relationship between a particular force/interaction and melting point to be controversial, considering the sum of different interactions is more reasonable, but this will cause complexity in analysis and lead to differences for different ILs. Analyzing the melting points of ILs from the thermodynamic perspective is reasonable and easy, which provides an identical conclusion for different ILs. GCM, QSPR, and COSMO-RS were proposed from macro, micro, and thermodynamic perspectives, respectively. Among them, the COSMO-RS shows the worst predicted performance, but from the theoretical perspective, more factors have been considered and it has a more theoretical basis. To further develop a theory model, COSMO-RS is the best choice among them. The original COSMO-RS model still has some problems, i.e., lacking some key physical characteristic variables to describe enthalpy and entropy of transition of ILs. Combining COSMO-RS with machine learning will be a promising way to further develop a quantitative model.

## Data availability statement

The original contributions presented in the study are included in the article/Supplementary Material; further inquiries can be directed to the corresponding author.

## Author contributions

Conceptualization: X. Ji and X. Lu; Software: X. Lu; Investigation: Z. Dai and L. Wang; Writing—original draft preparation: Z. Dai and L. Wang; Writing—review and editing: X. Ji and X. Lu; Visualization: Z. Dai and L. Wang. All authors contributed to the article and approved the submitted version.

## CRedit authorship contribution statement

**Zhengxing Dai:** Writing – review & editing, Writing – original draft, Visualization, Investigation. **Lei Wang:** Writing

– original draft, Visualization, Investigation, Data curation. **Xiaohua Lu:** Writing – review & editing, Supervision, Software, Funding acquisition, Conceptualization. **Xiaoyan Ji:** Writing – review & editing, Supervision, Software, Funding acquisition, Conceptualization.

## Conflict of interest

The authors declare that the research was conducted in the absence of any commercial or financial relationships that could be construed as a potential conflict of interest.

## Acknowledgments

We would like to thank the financial support from National Natural Science Foundation of China (No. 21838004, 22011530112), China Scholarship Council (No. 202208320253), STINT (CH2019-8287), and the Swedish Research Council. X. Ji thanks the financial support from Horizon-EIC, Pathfinder challenges, Grant Number: 101070976.

## Appendix A. Supplementary data

Supplementary data to this article can be found online at <https://doi.org/10.1016/j.gee.2024.01.009>.

## References

- [1] S. Zhang, J. Zhang, Y. Zhang, Y. Deng, *Chem. Rev.* 117 (2017) 6755–6833.
- [2] Y. Chen, Y. Sun, Z. Yang, X. Lu, X. Ji, *Appl. Energy* 257 (2020) 113962.
- [3] C. Ma, A. Laaksonen, C. Liu, X. Lu, X. Ji, *Chem. Soc. Rev.* 47 (2018) 8685–8720.
- [4] Z. Dai, Y. Chen, Y. Sun, Z. Zuo, X. Lu, X. Ji, *Front. Chem.* 10 (2022) 941352.
- [5] D.D. Patel, J.M. Lee, *Chem. Rec.* 12 (2012) 329–355.
- [6] D.R. Macfarlane, N. Tachikawa, M. Forsyth, J.M. Pringle, P.C. Howlett, G.D. Elliott, J.H. Davis, M. Watanabe, P. Simon, C.A. Angell, *Energy Environ. Sci.* 7 (2014) 232–250.
- [7] C.L. Aguirre, L.A. Cisternas, J.O. Valderrama, *Int. J. Thermophys.* 33 (2011) 34–46.
- [8] W. Cao, B. Senthikumar, V. Causin, V.P. Swamy, Y. Wang, G. Saielli, *Soft Matter* 16 (2020) 411–420.
- [9] S. Naserifar, A. Koschella, T. Heinze, D. Bernin, M. Hasani, *RSC Adv* 13 (2023) 18639–18650.
- [10] M.A. Zakharov, Y.V. Filatova, S.R. Mikheeva, M.A. Bykov, N.V. Avramenko, V.A. Tafeenko, *Russ Chem Bull* 71 (2022) 1240–1246.
- [11] Y. Zhang, E.J. Maginn, *J. Chem. Phys.* 136 (2012) 144116.
- [12] B. Sepehri, *J. Mol. Liq.* 297 (2020) 112013.
- [13] V. Villazón-León, A. Bonilla-Petriciolet, J.C. Tapia-Picazo, J.G. Segovia-Hernández, M.L. Corazza, *Chem Eng Res Des* 185 (2022) 458–480.
- [14] D.K. Mital, P. Nancarrow, S. Zeinab, N.A. Jabbar, T.H. Ibrahim, M.I. Khamis, A. Taha, *Molecules* 26 (2021) 2454.
- [15] V. Venkatraman, S. Evjen, H.K. Knuutila, A. Fiksdahl, B.K. Alsberg, *J. Mol. Liq.* 264 (2018) 318–326.
- [16] O.D. Gupta, B. Twamley, J.N.M. Shreeve, *Tetrahedron Lett* 45 (2004) 1733–1736.
- [17] P. González-Izquierdo, O. Fabelo, I. Cano, O. Vallcorba, J. Rodríguez Fernández, M.T. Fernández-Díaz, I. De Pedro, *J. Mol. Liq.* 325 (2021) 114570.

- [18] S.L. Wang, W.L. Yuan, Y. Zhao, K.L. Cheng, G.H. Tao, L. He, Dalton Trans 52 (2023) 8975–8985.
- [19] A.V. Agafonov, N.O. Kudryakova, L.M. Ramenskaya, E.P. Grishina, Arab. J. Chem. 13 (2020) 9090–9104.
- [20] L. Liu, J. Bai, Z. Su, Y. Yao, Z. Zhou, Y. Xia, Y. Zhang, ACS Omega 8 (2023) 16738–16747.
- [21] P.D. Diabate, L. Boulafrouh, S. Boudesocque, L. Dupont, A. Mohamadou, Sep Sci Technol 58 (2023) 1689–1702.
- [22] A.E. Langtry, K.B. Thompson, N.D. Redeker, A.S. Quintana, D.L. Bui, K.T. Greeson, N. Cena, J.C. Marcischak, L.M.J. Moore, K.B. Ghiassi, J. Mol. Liq. 359 (2022) 119282.
- [23] T. Myrdek, C. Popescu, W. Kunz, J. Mol. Liq. 322 (2021) 114947.
- [24] R.A. O'brien, P.C. Hillesheim, M. Soltani, K.J. Badilla-Nunez, B. Siu, M. Musozoda, K.N. West, J.H. Davis Jr., A. Mirjafari, J. Phys. Chem. B 127 (2023) 1429–1442.
- [25] A. Warrington, C.S.M. Kang, C. Forsyth, C.M. Doherty, D. Acharya, L.A. O'dell, N. Sirigiri, J.W. Boyle, O.E. Hutt, M. Forsyth, J.M. Pringle, Mater. Chem. Front. 6 (2022) 1437–1455.
- [26] S. Lerch, T. Strassner, Chem. Eur. J. 27 (2021) 15554–15557.
- [27] E. Del Río, T. Vidil, W. Gati, É. Grau, D. Taton, H. Cramail, ACS Sustain. Chem. Eng. 9 (2021) 12687–12698.
- [28] T. Peppel, M. Kockerling, Materials 14 (2021) 2676.
- [29] R. Kawai, M. Niki, S. Yada, T. Yoshimura, Colloids Surf. A Physicochem. Eng. Asp. 603 (2020) 125218.
- [30] L. Darabi, M. Zare, New J. Chem. 44 (2020) 4023–4032.
- [31] E.A. Turner, C.C. Pye, R.D. Singer, J. Phys. Chem. A 107 (2003) 2277–2288.
- [32] C.A. Cassity, B. Siu, M. Soltani, J.L. Mcgeehee, K.J. Strickland, M. Vo, E.A. Salter, A.C. Stenson, A. Wierzbicki, K.N. West, B.D. Rabideau, J.H. Davis, Phys. Chem. Chem. Phys. 19 (2017) 31560–31571.
- [33] B.D. Rabideau, M. Soltani, R.A. Parker, B. Siu, E.A. Salter, A. Wierzbicki, K.N. West, J.H. Davis Jr., Phys. Chem. Chem. Phys. 22 (2020) 12301–12311.
- [34] B. Khalili, M.P. Amani, K. Ghauri, J. Fluor. Chem. 261–262 (2022) 110026.
- [35] X.M. Chen, X. Jiang, Y. Jing, X. Chen, Chem. Asian. J. 16 (2021) 2475–2480.
- [36] O. Terenteva, A. Bikmukhametov, A. Gerasimov, P. Padnya, I. Stoikov, Molecules 27 (2022) 8006.
- [37] R. Sumitani, T. Mochida, J. Mol. Liq. 344 (2021) 117784.
- [38] M. Niemczak, L. Sobiech, M. Grzanka, J. Agric. Food Chem. 68 (2020) 13661–13671.
- [39] H. Yoon, S. Shin, S. Park, M.W. Shin, J. Mol. Liq. 359 (2022) 119352.
- [40] H. Abe, S. Kobayashi, K. Ogawa, K. Imai, K. Koshiji, M. Hoshino, T. Hirano, Y. Hata, H. Kishimura, M. Uruichi, Chem. Phys. 570 (2023) 111872.
- [41] P.S. Borchers, P. Gerlach, Y. Liu, M.D. Hager, A. Balducci, U.S. Schubert, Energies 14 (2021) 6344.
- [42] E. Fabre, S.M.S. Murshed, J. Mater. Chem. A 9 (2021) 15861–15879.
- [43] B. O'rouke, C. Lauderback, L.I. Teodoro, M. Grimm, M. Zeller, A. Mirjafari, G.L. Guillet, P.C. Hillesheim, ACS Omega 6 (2021) 32285–32296.
- [44] X. Tang, D. Xiao, Z. Xu, Q. Liu, B. Ding, H. Dou, X. Zhang, J. Mater. Chem. A 10 (2022) 18374–18382.
- [45] A. Zafar, D. Imtiaz Ud, R.G. Palgrave, H. Muhammad, S. Yousuf, T. Evans, ChemistryOpen 12 (2023) e202200229.
- [46] T. Huang, W. Zhao, X. Zhang, X. Nie, J. Chen, W. Xiong, J. Mol. Liq. 320 (2020) 114465.
- [47] J. Liu, W. Yang, Z. Li, F. Ren, H. Hao, J. Mol. Liq. 307 (2020) 112994.
- [48] J.P. Sethna, Statistical mechanics: entropy, order parameters, and complexity, second ed., Oxford, New York, 2006.
- [49] T. Endo, K. Sunada, H. Sumida, Y. Kimura, Chem. Sci. 13 (2022) 7560–7565.
- [50] K. Padaszyński, K. Kłębowski, M. Królikowska, J. Mol. Liq. 344 (2021) 117631.
- [51] D.K. Mital, P. Nancarrow, T.H. Ibrahim, N. Abdel Jabbar, M.I. Khamis, Ind. Eng. Chem. Res. 61 (2022) 4683–4706.
- [52] K.C. Lethesh, K. Van Hecke, L. Van Meervelt, P. Nockemann, B. Kirchner, S. Zahn, T.N. Parac-Vogt, W. Dehaen, K. Binnemans, J. Phys. Chem. B 115 (2011) 8424–8438.
- [53] T. Gharehdaghi, J. Karimi-Sabet, S.M. Ghoreishi, M. Motallebipour, S. Sadjadi, J. Mol. Liq. 345 (2022) 118174.
- [54] D.M. Eike, J.F. Brennecke, E.J. Maginn, Green Chem 5 (2003) 323–328.
- [55] A.R. Katritzky, A. Lomaka, R. Petrukhin, R. Jain, M. Karelson, A.E. Visser, R.D. Rogers, J. Chem. Inf. Comput. Sci. 42 (2002) 71–74.
- [56] A.R. Katritzky, R. Jain, A. Lomaka, R. Petrukhin, M. Karelson, A.E. Visser, R.D. Rogers, J. Chem. Inf. Comput. Sci. 42 (2002) 225–231.
- [57] C. Yan, M. Han, H. Wan, G. Guan, Fluid Phase Equilib 292 (2010) 104–109.
- [58] N. Sun, X. He, K. Dong, X. Zhang, X. Lu, H. He, S. Zhang, Fluid Phase Equilib 246 (2006) 137–142.
- [59] Y. Ren, J. Qin, H. Liu, X. Yao, M. Liu, QSAR Comb. Sci. 28 (2009) 1237–1244.
- [60] I. Lopez-Martin, E. Burello, P.N. Davey, K.R. Seddon, G. Rothenberg, Chemphyschem 8 (2007) 690–695.
- [61] J.S. Torrecilla, F. Rodríguez, J.L. Bravo, G. Rothenberg, K.R. Seddon, I. Lopez-Martin, Phys. Chem. Chem. Phys. 10 (2008) 5826–5831.
- [62] N. Farahani, F. Gharagheizi, S.A. Mirkhani, K. Tumba, Thermochim. Acta 549 (2012) 17–34.
- [63] F. Yan, S. Xia, Q. Wang, Z. Yang, P. Ma, The J. Chem. Thermodyn. 62 (2013) 196–200.
- [64] P. Gantzer, B. Creton, C. Nieto-Draghi, Mol. Inform. 39 (2020) e1900087.
- [65] Y. Huo, S. Xia, Y. Zhang, P. Ma, Ind. Eng. Chem. Res. 48 (2009) 2212–2217.
- [66] F. Gharagheizi, P. Ilani-Kashkouli, A.H. Mohammadi, Fluid Phase Equilib 329 (2012) 1–7.
- [67] J.A. Lazzús, Fluid Phase Equilib 313 (2012) 1–6.
- [68] Y. Chen, G.M. Kontogeorgis, J.M. Woodley, Ind. Eng. Chem. Res. 58 (2019) 4277–4292.
- [69] K.G. Joback, R.C. Reid, Chem. Eng. Commun. 57 (2007) 233–243.
- [70] L. Zhao, S.H. Yalkowsky, Ind. Eng. Chem. Res. 38 (1999) 3581–3584.
- [71] R.-M. Dannenfelser, S.H. Yalkowsky, Ind. Eng. Chem. Res. 35 (1996) 1483–1486.
- [72] U. Preiss, S. Bulut, I. Krossing, J. Phys. Chem. B 114 (2010) 11133–11140.
- [73] J. Willard, X. Jia, S. Xu, M. Steinbach, V. Kumar, ACM Comput. Surv. 55 (66) (2022) 1–66, 37.